Published in final edited form as:
J Cereb Blood Flow Metab. 2009 August ; 29(8): 1482–1490. doi:10.1038/jcbfm.2009.67.

Nonischemic cerebral venous hypertension promotes a pro-angiogenic stage via HIF-1 downstream genes and leukocyte-derived MMP-9

Peng Gao, PhD, MD[1,4,6], **Yiqian Zhu, MD**[1], **Feng Ling, MD**[4], **Fanxia Shen, MD**[1], **Brian Lee, BA**[1], **Rodney Allanigue Gabriel, BS**[1], **Qi Hao, PhD**[1], **Guo-Yuan Yang, MD, PhD**[1,5], **Hua Su, MD**[1], and **William L. Young, MD**[1,2,3]

[1]Center for Cerebrovascular Research, Department of Anesthesia and Perioperative Care, University of California,San Francisco, CA

[2]Department of Neurological Surgery, University of California, San Francisco, CA

[3]Department of Neurology, University of California, San Francisco, CA

[4]Department of Neurosurgery, Xuanwu Hospital, Capital University of Medical Sciences, Beijing, China

[5]Med-X Research Institute, Shanghai JiaoTong University, Shanghai, China

[6]Department of Neurosurgery, Tongji Hospital, Tongji University, Shanghai, China

Abstract

Cerebral venous hypertension (VH) and angiogenesis are implicated in the pathogenesis of brain arteriovenous malformation and dural arteriovenous fistulae. We studied the association of VH and angiogenesis using a mouse brain VH model. Sixty mice underwent external jugular vein and common carotid artery (CCA) anastomosis (VH model), CCA ligation, or sham dissection (n=20). Hypoxia-inducible factor-1α (HIF-1α), vascular endothelial growth factor (VEGF) and stromal cell-derived factor-1α (SDF-1α) expression, and matrix metalloproteinase (MMP) activity were analyzed. We found VH animals had higher ($p<0.05$) SSP pressure (8±1 mmHg) than control groups (1±1 mmHg). Surface cerebral blood flow and mean arterial pressure did not change. HIF-1, VEGF and SDF-1α expression increased ($p<0.05$). Neutrophils and MMP-9 activity increased 10-fold 1 day after surgery, gradually decreased afterwards, and returned to baseline 2 weeks after surgery. Macrophages began to increase 3 days after surgery ($p<0.05$), which coincided with the changes in SDF-1α expression. Capillary density in the parasagittal cortex increased 17% compared to the controls. Our findings suggest that mild nonischemic VH results in a pro-angiogenic stage in the brain by upregulating HIF-1 and its downstream targets, VEGF and SDF-1α, increasing leukocyte-infiltration and MMP-9 activity.

Keywords

Mouse brain venous hypertension; HIF-1; MMP-9; angiogenesis; inflammatory cells

Correspondence: Hua Su, MD University of California, San Francisco Department of Anesthesia and Perioperative Care 1001 Potrero Ave, Room 3C-38 San Francisco, CA 94110 Tel: 415-206-3162; Fax: 415-206-8907 hua.su@ucsf.edu.

Disclosure/conflict of interest The authors state no conflict of interest.

Introduction

Angiogenesis is involved in the pathogenesis of brain arteriovenous malformation (BAVM) (Hashimoto *et al*, 2005) and dural arteriovenous fistulae (DAVF) (Lawton *et al*, 1997). Clinically, patients with intracranial arteriovenous shunting within BAVM or DAVF usually have complications related to venous hypertension (VH). However, the contribution of these aberrant hemodynamic changes to the lesion formation or progression is poorly understood.

It has been shown that vascular endothelial growth factor (VEGF) increases in both surgically resected dural sinuses harboring DAVF (Uranishi *et al*, 1999) and brain AVM samples (Hatva *et al*, 1996; Koizumi *et al*, 2002). Ng et al (Ng *et al*, 2005) and Sure et al (Sure *et al*, 2004) demonstrated that expression of hypoxia-inducible factor-1 (HIF-1) is significantly correlated to VEGF expression in human AVM, suggesting that HIF-1 plays a role in the induction and maintenance of angiogenesis and vascular remodeling in brain AVM. Increases of VEGF expression and brain microvascular density have also been shown in the brains with VH in animal models (Hai *et al*, 2003; Lawton *et al*, 1997; Shin *et al*, 2003; Zhu *et al*, 2006).

Inflammatory cells participate in tissue angiogenesis by releasing pro-angiogenic factors and cytokines, including matrix metalloproteinases (MMPs). Inflammatory cell infiltration, as well as their subsequent release of MMPs, may play a role in the angiogenic process in the brain with VH by enhancing the invasion and migration of endothelial cells and macrophages through the surrounding basement membrane and extracellular matrix (ECM).

Chemokines are a group of structurally related, small (8-14 kDa) polypeptide signaling molecules that can induce the adhesion, migration, and activation of diverse cell types. Recently, stromal-cell-derived factor-1α (SDF-1α or CXCL12a) has been reported to be a critical mediator in inflammation and angiogenesis. SDF-1α, a strong chemotactic factor, can activate a broad spectrum of leukocytes, including monocytes, neutrophils, and hematopoietic progenitor cells (Aghi *et al*, 2006; Petit *et al*, 2007). Du et al (Du *et al*, 2008) demonstrated that HIF-1, partly through the increases in VEGF and SDF-1α, induces recruitment of $CD45^+$ bone marrow-derived cells (BMDCs) to promote angiogenic activity in the brain tumor, and that MMP-9 activity is essential in initiating angiogenesis by increasing VEGF bioavailability. SDF-1α can also enhance tumor angiogenesis indirectly, by inducing the secretion of several angiogenic factors including VEGF (Ping *et al*, 2007).

Several animal models manifesting lesions resembling VH have been well developed and have helped address specific interventional issues, but most of them were created in rats. The relationship of angiogenesis and brain VH has not been clarified using these models. In order to clarify the causal relationship between VH and angiogenesis, we developed a mouse VH model. We showed that VH in an HIF-1-dependent manner promotes angiogenesis and leukocyte infiltration via increases in VEGF, SDF-1α, and MMP-9 expression under nonischemic conditions, providing a link between VH and angiogenic activities.

Materials and methods

Experimental Design

Animal procedures were approved by the Committee on Animal Research at the University of California, San Francisco. A total of 60 male C57BL/6J mice, weighing 25 and 30 g, were randomly separated into 3 groups: 20 VH, 20 sham-operated and 20 with common carotid artery (CCA) ligation. Mice were sacrificed at 1, 3, 7, and 14 days after surgery. Hemodynamic measurements were made pre- and post-surgery, and brains were harvested.

Surgical Procedure

Mice were anesthetized with intra-peritoneal injections of ketamine (100 mg/kg) and xylazine (10 mg/kg). Through an anterior midline cervical incision, the right CCA was exposed from its bifurcation down to the clavicle. The external jugular vein (EJV) in the subcutaneous tissue was exposed from the cranial base down to the clavicle. CCA and EJV were trapped with temporary aneurysm clips and transected. Proximal CCA was connected to the cranial stump of EJV with end-to-end anastomosis performed under an operating microscope with continuous 11-0 monofilament nylon sutures (MONOSOF, Synecture). The distal CCA and caudal stump of EJV were occluded with bipolar cauterization (Figure 1A, 1B, and 1C). All incisions were closed with a 6-0 nylon suture (MONOSOF, Synecture). Forty mice without CCA and EJV anastomosis were used as controls; 20 underwent sham surgery (midline neck exploration) and 20 underwent left carotid artery occlusion.

Hemodynamic Measurement

Mean arterial pressure (MBP), sagittal sinus pressure (SSP), and surface cortex cerebral blood flow (CBF) were measured pre- and post-operation. MBP was measured non-invasively using tail cuff and pulse transducer system (NIBP, AD Instruments, CO). SSP was documented by cannulating a 30-gauge needle connected to a pressure transducer and signal amplifier (PowerLab, Colorado Springs, CO). Surface CBF was measured using a laser Doppler probe (Laserflo BPM^2, Vasomedics, St. Paul, MN) that penetrates brain tissue approximately 1 mm beyond the probe ending. The probe was placed on the surface of the parasagittal parietal cortex. Means of four serial measurements made on each side were documented.

Immunohistochemistry

For single-label immunohistochemistry, 20 μm thick coronal brain sections were fixed in 4% paraformaldehyde (PFA) for 15 minutes and quenched in 0.3% H_2O_2 with methanol for 30 minutes. After blocking in 5% goat serum for 30 minutes, sections were incubated with primary antibodies at the following concentrations: rabbit anti-mouse myeloperoxidase (MPO), 1:200 (Lab Vision); rat anti-mouse CD68, 1:50 (Serotec); rabbit anti-mouse MMP-9, 1:150 (Chemicon); SDF-1 rabbit anti-mouse, 1:200 (eBioscience); VEGF rabbit anti-mouse, 1:100 (Santa Cruz Biotechnology); and HIF-1α anti-mouse, 1:100 (Novus Biologicals). After incubating at 4°C overnight, the sections were incubated with biotinylated secondary antibodies for 1.5 hours at room temperature, and were treated with the ABC streptavidin detection system (Vector Lab) for 1.5 hours. The resulting horseradish peroxidase signal was detected using 3, 3′-diaminobenzidene.

For double fluorescent staining, after incubating at 4°C overnight with primary antibodies, sections were incubated with Alexa Fluor 594- or 488-conjugated labeling (Invitrogen) for 1.5 hours at room temperature. They were then mounted and photographed with a fluorescent microscope. Negative controls were performed by omitting the primary antibodies during the immunostaining. The numbers of neutrophils (MPO positive) and macrophage (CD68 positive) were counted blindly in 5 coronal sections of each animal under a high-power (200X) Leica microscope with a digital camera. For microvessel counting in the parasagittal cortex region, the sections were stained with *fluoresceinlycopersicin esculentum lectin* (Vector Lab). Vessel density was counted in 5 coronal sections per animal using NIH Image 1.63 software (National Institutes of Health, Bethesda, MD).

Gelatin Zymography

The protein isolated from the parasagittal cortex was separated under non-reducing conditions in a 10% zymogram gel (Invitrogen) containing 0.1% gelatin as a substrate. Following electrophoresis, gels were washed and incubated overnight in developing buffer at 37°C. Then

the gels were stained with 0.5% Coomassie Blue R-250 (Bio-Rad Laboratories) and de-stained. MMP activity could be detected as white bands against the Coomassie blue stained gel. Recombinant MMP-9 and MMP-2 (Chemicon) were run in the same gel as references. Gelatinolytic bands were quantified using densitometry and analyzed using NIH Image 1.63 software.

Western Blot Analysis

Aliquots of the proteins for gelatin zymography were used for Western blot analysis. Proteins were separated in 14% of Tris-Glycine gel and electrotransferred onto a nitrocellulose membrane (Bio-Rad Laboratories) in transfer buffer (Invitrogen) by semidry blotting. After blocking in 5% milk, the membrane was incubated with rabbit anti-mouse VEGF antibody (1:200, Santa Cruz Biotechnology) overnight at 4°C. After washing, the membrane was incubated with horseradish peroxidase conjugated anti-rabbit secondary antibody (Amersham, Buckinghamshire, UK) diluted at 1:10,000, and then reacted with FEMO detection reagent (Pierce Biotechnology). The membrane was exposed to Kodak film, and developed according to the manufacturer's instructions. VEGF expressions were analyzed by optical density using NIH Image 1.63 software.

SDF-1 Enzyme-linked Immunosorbent Assay (ELISA)

The protein isolated from the parasagittal cortex was collected and stored at -80°C until assayed. The SDF-1α level was measured by ELISA using a commercial kit (Mouse SDF-1α ELISA kit, MCX120, R&D Systems) according to the manufacturer's instructions.

Statistical Analyses

Data are presented as mean ± standard deviation. Means were compared using one-way ANOVA analysis followed by the post hoc *t* test. A probability value of less than 0.05 was considered statistically significant.

Results

SSP Increased Dramatically in Mice with CCA and EJV Anastomosis

To analyze if the CCA and EJV connection caused brain VH and other hemodynamic changes, we measured SSP, CBF and MBP before and after surgery. We found that the connection resulted in immediate and sustained increase of venous pressure in the mouse brains, with 4 to 6-fold elevations in SSP. In contrast, sham surgery and CCA-ligation did not result in VH in the brains ($p<0.05$, Figure 1D). No differences were observed in CBF before and after surgery among the groups, indicating that we created a nonischemic brain VH (Figure 1E). There were also no significant differences in MBP between VH and control mice pre- and post-operation (Figure 1F). Thus, the CCA-EJV connection increased venous pressure in the brains without compromising cerebral and systemic blood flow (no ischemia).

HIF-1α Expression Increased in Response to VH

To analyze if nonischemic VH increased HIF-1α expression in the brain, we determined HIF-1α protein in the VH brain using immunohistochemical staining. We found that HIF-1α increased in the endothelial cells at the parasagittal cortex 1 day after the onset of VH (Figure 2A). HIF-1α expression was minimal in the brains of mice subjected to sham surgery or CCA-ligation. Thus, nonischemic VH increased HIF-1α proteins in the brain.

HIF-1 Target Genes, VEGF and SDF-1α Increased in VH Brains

To study if increased HIF-1 activity in the VH brain upregulated its downstream gene (VEGF), we analyzed VEGF expression using immunostaining and Western blot. The results showed

that VEGF expression was higher in the parasagittal cortex region of VH mice than that of control mice (Figure 2A). Double fluorescence staining using lectin and VEGF-specific antibody showed that VEGF was expressed by endothelial cells (Figure 2A). VEGF expression began to increase at day 3, peaked at day 7, and decreased 2 weeks following surgery (Figure 2B). There was significantly more VEGF in the brains of VH mice than in the brains of mice without VH ($p<0.05$) (Figure 2B). In addition, we observed higher vascular density in the VH brain than in control brains 2 weeks after surgery; however, the differences did not reach a statistically significant level (data not shown).

SDF-1α is another HIF-1 downstream gene that promotes angiogenesis by attracting bone marrow-derived mononuclear cells homing to the angiogenic focus (Hiasa *et al*, 2004), and induces secretion of the angiogenic factor (De Falco *et al*, 2004; Petit *et al*, 2007). We found that SDF-1α expression was up-regulated in the parasagittal cortex adjacent to the sagittal sinus of HV mice. Minimum SDF-1α-positive signal was detected in control brains (Figure 2A). Double fluorescence staining showed that SDF-1α was mainly expressed by endothelial cells (Figure 2A). ELISA analysis demonstrated that, similar to VEGF, SDF-1α expression also increased 3 days, peaked 1 week, and decreased 2 weeks after surgery (Figure 2C). These findings indicate that SDF-1 was also involved in pro-angiogenic changes in the VH brain.

Neutrophil-associated MMP-9 Activities Increased in Response to VH

To test whether increased VEGF and SDF-1α expression in VH brains resulted in the recruitment of bone marrow-derived mononuclear cells, we quantified neutrophils in VH brains by immunostaining using MPO-specific antibody. We found that the number of neutrophils increased significantly in the VH brain 1 day following surgery, while minimal neutrophils were found in the control brains ($p<0.05$, Figure 3B). The MPO-positive cells were mainly located at the vessel wall in the tissues close to the midline, such as the parasagittal cortex, and to a lesser degree in the basal ganglia (Figure 3A). The number of neutrophils peaked 1 day after surgery, gradually decreased, and returned to the baseline after 2 weeks of surgery (Figure 3B).

Since inflammatory cells participate in angiogenesis by producing MMPs(Coussens *et al*, 2000), we analyzed MMP-2 and MMP-9 activity in the VH brain using zymography. MMP-9 activity was most prominent at day 1, remained high for more than 1 week, and then returned to the baseline 2 weeks after surgery (Figure 3C and 3D). In the control groups, minimal MMP-9 activity was observed. MMP-2 was equally expressed in all the groups at all time points. The MMP-9 was colocalized with neutrophils (Supplementary Figure 1) and the time course of MMP-9 expression coincided with the neutrophil infiltration, indicating that MMP-9 was neutrophil-derived and that it may play a role in early response to shear stress changes, facilitating subsequent inflammatory events such as macrophage infiltration.

Macrophages Increased in Response to VH

Macrophages have also been shown to participate in angiogenesis. To investigate whether the monocyte/macrophages were recruited in VH brains, we performed immunohistochemical staining using CD68-specific antibody. We found that the number of microphages increased significantly in the VH brain 3 days after surgery (Figure 3E and 3G). The $CD68^+$ cells were found in the parasagittal cortex, including frontal, parietal, and occipital lobes, and, to a lesser degree, in the basal ganglia. The increase of $CD68^+$ cells sustained for more than 2 weeks post surgery ($p<0.05$, Figure 3E). The time course of macrophages coincided with SDF-1α expression, suggesting that the microphages were attracted by SDF-1α. Furthermore, immunofluorescence staining showed that $CD68^+$ cells were located on the vessel wall as well as the parenchyma of the VH brains (Figure 3F).

Discussion

This study reports the first cerebral VH murine model. In this model, SSP increased 4 to 6-fold, while CBF and MBP did not change, indicating a nonischemic brain VH. We found that: (1) the presence of VH increased HIF-1 and its downstream targets, VEGF and SDF-1α expression, in the parasagittal cortex of the mouse brain; (2) leukocytes, including neutrophils and macrophages, were recruited to the parasagittal cortex; (3) MMP-9 activity increased and MMP-9 protein co-localized with neutrophils--MMP-9 activity peaked with the number of neutrophils in VH brains 1 day after the surgery; (4) the macrophage infiltration began 3 days after surgery, coinciding with the time course of SDF-1α expression in endothelial cells; and (5) there was a trend of microvessel density increase in VH brains at 2 weeks after surgery. Our current findings suggest that the pro-angiogenic stage in VH brains is promoted by HIF-1-upregulated VEGF and SDF-1 expression and leukocyte infiltration. Thus, HIF-1 downstream genes (VEGF and SDF-1) and leukocytes play critical roles in the mechanism that links brain VH and angiogenesis. Furthermore, these factors induced by VH may facilitate vascular remodeling, and participate in the pathogenesis associated with VH in the human brain. VH is commonly thought to exert its deleterious effect on the brain by a simple reduction in cerebral perfusion pressure resulting in cerebral ischemia. Our studies point to an additional and underappreciated set of physiological effects that are caused by nonischemic levels of venous pressure.

Our mouse brain VH model was created by a CCA-EJV fistula, which resulted in a sustained increase of SSP in the brain. None of the mice with cerebral VH showed behavioral changes or neurological dysfunction associated with ischemia. In this model, the hemodynamics, including surface cortex CBF and systematic MBP, did not significantly change, which suggested that VH did not compromise cerebral perfusion. Thus, the increased HIF-1 expression in our brain VH model was due to mechanisms other than ischemia, such as endothelial share stress.

HIF-1 has been proposed as a key factor that upregulates the expression of SDF-1 and VEGF. These two factors recruit MMP-9-bearing bone marrow-derived cells to participate in tumor angiogenesis of the mouse brain (Aghi *et al*, 2006; Du *et al*, 2008; Hao *et al*, 2008; Lyden *et al*, 2001). In this study, we demonstrated that focal hemodynamic derangement in the brain resulted in recruitment of MPO-positive leukocytes to endorse angiogenesis. Circulating neutrophils responded to brain VH earlier than macrophages. The number of neutrophils peaked 1 day following surgery. MMP-9 activity increased in the same region at the same time. Immunostaining showed that MMP-9 was expressed by neutrophils in the vessel wall, which is consistent with findings in human BAVM samples (Chen *et al*, 2008). MMP-9 produced by neutrophils may facilitate the degradation of the extracellular matrix (ECM), and thus promote the invasion and migration of endothelial cells, as well as monocytes through the surrounding basement membrane and ECM (Philip *et al*, 2004). In addition, MMP-9 can release VEGF from ECM, which results in the initiation of angiogenesis (Bergers *et al*, 2000; Page-McCaw *et al*, 2007). Macrophage infiltration increased 3 days after surgery, which is chronologically correlated with the increase of SDF-1 expression. Based on the immunohistochemistry analysis, macrophages were located both in the vessel wall and brain parenchyma. This finding is consistent with the previous report (Chen *et al*, 2008) for human BAVM tissue, and supports the notion that VH induces leukocyte infiltration. VEGF and SDF-1α expression peaked 1 week post-operation. Both of these factors are expressed by endothelial cells and play a pivotal role in attracting circulating leukocytes homing to angiogenic foci. SDF-1 may mediate the retention of circulating leukocytes in close proximity to angiogenic vessels (De Falco *et al*, 2004; Petit *et al*, 2007). Inflammatory cells also enhance local in situ proliferation of endothelial cells via secretion of pro-angiogenic cytokines. Taken together, our findings

suggest that nonischemic VH conditions may upregulate the expression of HIF-1 and its downstream genes, VEGF and SDF-1, and facilitate the recruitment of leukocytes.

Brain VH occurs in several human diseases, such as BAVM. The fundamental defect in human BAVM is high-flow arteriovenous shunting, frequently accompanied by VH shown as venous outflow restriction and aberrant venous drainage patterns by angiography. The importance of raised venous pressure in the pathophysiology of AVMs has gained recognition, and the pathogenesis of vascular lesions is closely linked to angiogenesis. In certain cases, active angiogenesis might be a part of the underlying pathophysiology of the growth and regression of BAVM (Du *et al*, 2007; Nussbaum *et al*, 1998). In response to VH, endothelial cells are subject to a high intravascular shear stress that is able to convert mechanical stimuli into molecular events, e.g., upregulation of HIF-1α as well as its downstream expressions. It provides a bridge that links HIF-1 and pro-angiogenic stage in response to VH.

In the clinical setting, VH is commonly associated with brain injury because it decreases cerebral perfusion pressure, resulting in ischemic damage. Our results show that even modest levels of VH have a pro-angiogenic effect that can influence the course of diseases in the absence of ischemia. The pro-angiogenic effect of VH has also been observed in the pathogenesis of other diseases. Intracranial hypertension (IH) is often accompanied by increased cerebrospinal fluid (CSF) pressure within the skull. Elevated CSF pressure compresses the veins, which then results in venous outflow obstruction and VH. Koehne et al (Koehne *et al*, 2002) examined 57 CSF aliquots obtained from patients with hydrocephalus, and found that IH may trigger release of VEGF into CSF. In addition, VH has been implicated in dural arteriovenous fistula (DAVF) (Bederson *et al*, 1991; Herman *et al*, 1995; Kusaka *et al*, 2001; Terada *et al*, 1994). All of the evidence above highlight the importance of VH in the development and recurrence of vascular lesions.

Pro-angiogenic activities have also been identified in rat VH brain models (Shin *et al*, 2003). Hai et al (Hai *et al*, 2002; Hai *et al*, 2003) observed increased capillary density in the rat brains at day 7 following surgery, and this increase was maintained for up to 3 months. We have found in our previous study with a rat model that nonischemic brain VH increases HIF-1 and VEGF expression, and proposed a possible role of HIF-1 in the induction of angiogenesis in VH brains (Zhu *et al*, 2006). The present study provides an important extension of the prior work by our groups and others, by showing that in addition to increased VEGF, SDF-1α, another HIF-1 downstream gene that participates in tissue angiogenesis, increased in the VH brain. We have also observed leukocyte infiltration and increased MMP-9 activity. The emerging picture that comes into view is that VH exerts its pro-angiogenic effects through VEGF, SDF-1α and MMP-9 released by leukocytes.

Recently, genetic mutant mice were used in research to generate BAVM that mimics human BAVM, including mice with endoglin (ENG) (Satomi *et al*, 2003; Xu *et al*, 2004), activin-like kinase 1 (ALK1) (Park *et al*, 2008), or Notch (int3) (Carlson *et al*, 2005; Krebs *et al*, 2004; Murphy *et al*, 2008) haploinsufficiency. With brain VH in combination with genetic manipulation, a BAVM model that mimics human BAVM will likely be generated. The model will allow us to better understand the pathogenesis process of the disease and will serve as a testing model for the development of new therapies.

The major limitation of this study is that we did not measure arterial CO2 (PaCO2). However, the effect of the anesthetic and surgical preparation was similar among groups and the absolute level of PaCO2 or CBF was secondary to the fact that they were equivalent. The VH model has been mostly created on rats. The model by Zhu et al (Zhu *et al*, 2006), generated by a cervical fistula combined with the occlusion of transverse and sagittal sinuses, had a higher SSP over 20 mmHg. In contrast, our model was created by an arteriovenous fistula without

sinus occlusion. It may account for the mild increased SSP at 8 mmHg for our mouse model. The fact that the increased microvessels in the mouse VH brain did not reach statistically significant levels showed that the pro-angiogenic activity in the mouse VH brain is lower compared to that in the rat VH brain. We have attempted to reproduce rat surgical procedures in mice; however, the mice could not tolerate the procedures. Based on our experiment, we could not identify whether the leukocytes at the angiogenic site were derived from bone marrow. Future studies are needed to address the function of leukocytes in VH-induced angiogenesis. Finally, since neutrophil infiltration occurred earlier than the increase of SDF-1 and VEGF expression, further study is needed to identify the factors that cause the recruitment of neutrophils at the early time point.

In summary, our VH model was based on extradural A-V fistulas, which displayed pro-angiogenic features in the brain, including increased expression of HIF-1α and its downstream genes, VEGF and SDF-1α. Leukocyte infiltration was also observed. All of these results indicate that nonischemic level of VH, without compromising blood flow, can provide a pro-angiogenic environment in the brain that can be a mechanism for vascular remodeling in BAVM and other diseases associated with brain VH.

Supplementary Material

Refer to Web version on PubMed Central for supplementary material.

Acknowledgments

The authors thank Voltaire Gungab for editorial assistance and the staff of the Center for Cerebrovascular Research (http://avm.ucsf.edu/) for their collaborative support.

Funding This work was supported by the National Institutes of Health (NS27713 and NS044155 to WLY), and the American Heart Association (SDG 0535018N to HS).

References

Aghi M, Cohen KS, Klein RJ, Scadden DT, Chiocca EA. Tumor stromal-derived factor-1 recruits vascular progenitors to mitotic neovasculature, where microenvironment influences their differentiated phenotypes. Cancer Res 2006;66:9054–64. [PubMed: 16982747]

Bederson JB, Wiestler OD, Brustle O, Roth P, Frick R, Yasargil MG. Intracranial venous hypertension and the effects of venous outflow obstruction in a rat model of arteriovenous fistula. Neurosurgery 1991;29:341–50. [PubMed: 1922700]

Bergers G, Brekken R, McMahon G, Vu TH, Itoh T, Tamaki K, Tanzawa K, Thorpe P, Itohara S, Werb Z, Hanahan D. Matrix metalloproteinase-9 triggers the angiogenic switch during carcinogenesis. Nat Cell Biol 2000;2:737–44. [PubMed: 11025665]

Carlson TR, Yan Y, Wu X, Lam MT, Tang GL, Beverly LJ, Messina LM, Capobianco AJ, Werb Z, Wang R. Endothelial expression of constitutively active Notch4 elicits reversible arteriovenous malformations in adult mice. Proc Natl Acad Sci U S A 2005;102:9884–9. [PubMed: 15994223]

Chen Y, Zhu W, Bollen AW, Lawton MT, Barbaro NM, Dowd CF, Hashimoto T, Yang GY, Young WL. Evidence for inflammatory cell involvement in brain arteriovenous malformations. Neurosurgery 2008;62:1340–9. [PubMed: 18825001]

Coussens LM, Tinkle CL, Hanahan D, Werb Z. MMP-9 supplied by bone marrow-derived cells contributes to skin carcinogenesis. Cell 2000;103:481–90. [PubMed: 11081634]

De Falco E, Porcelli D, Torella AR, Straino S, Iachininoto MG, Orlandi A, Truffa S, Biglioli P, Napolitano M, Capogrossi MC, Pesce M. SDF-1 involvement in endothelial phenotype and ischemia-induced recruitment of bone marrow progenitor cells. Blood 2004;104:3472–82. [PubMed: 15284120]

Du R, Hashimoto T, Tihan T, Young WL, Perry V, Lawton MT. Growth and regression of an arteriovenous malformation in a patient with hereditary hemorrhagic telangiectasia: case report. J Neurosurg 2007;106:470–7. [PubMed: 17367071]

Du R, Lu KV, Petritsch C, Liu P, Ganss R, Passegue E, Song H, Vandenberg S, Johnson RS, Werb Z, Bergers G. HIF1alpha induces the recruitment of bone marrow-derived vascular modulatory cells to regulate tumor angiogenesis and invasion. Cancer Cell 2008;13:206–20. [PubMed: 18328425]

Hai J, Ding M, Guo Z, Wang B. A new rat model of chronic cerebral hypoperfusion associated with arteriovenous malformations. J Neurosurg 2002;97:1198–202. [PubMed: 12450044]

Hai J, Li ST, Lin Q, Pan QG, Gao F, Ding MX. Vascular endothelial growth factor expression and angiogenesis induced by chronic cerebral hypoperfusion in rat brain. Neurosurgery 2003;53:963–70. [PubMed: 14519228]

Hao Q, Liu J, Pappu R, Su H, Rola R, Gabriel RA, Lee CZ, Young WL, Yang GY. Contribution of bone marrow-derived cells associated with brain angiogenesis is primarily through leucocytes and macrophages. Arterioscler Thromb Vasc Biol 2008;28:2151–7. [PubMed: 18802012]

Hashimoto T, Wu Y, Lawton MT, Yang GY, Barbaro NM, Young WL. Co-expression of angiogenic factors in brain arteriovenous malformations. Neurosurgery 2005;56:1058–65. [PubMed: 15854255]

Hatva E, Jaaskelainen J, Hirvonen H, Alitalo K, Haltia M. Tie endothelial cell-specific receptor tyrosine kinase is upregulated in the vasculature of arteriovenous malformations. J Neuropathol Exp Neurol 1996;55:1124–33. [PubMed: 8939195]

Herman JM, Spetzler RF, Bederson JB, Kurbat JM, Zabramski JM. Genesis of a dural arteriovenous malformation in a rat model. J Neurosurg 1995;83:539–45. [PubMed: 7666234]

Hiasa K, Ishibashi M, Ohtani K, Inoue S, Zhao Q, Kitamoto S, Sata M, Ichiki T, Takeshita A, Egashira K. Gene transfer of stromal cell-derived factor-1alpha enhances ischemic vasculogenesis and angiogenesis via vascular endothelial growth factor/endothelial nitric oxide synthase-related pathway: next-generation chemokine therapy for therapeutic neovascularization. Circulation 2004;109:2454–61. [PubMed: 15148275]

Koehne P, Hochhaus F, Felderhoff-Mueser U, Ring-Mrozik E, Obladen M, Buhrer C. Vascular endothelial growth factor and erythropoietin concentrations in cerebrospinal fluid of children with hydrocephalus. Childs Nerv Syst 2002;18:137–41. [PubMed: 11981620]

Koizumi T, Shiraishi T, Hagihara N, Tabuchi K, Hayashi T, Kawano T. Expression of vascular endothelial growth factors and their receptors in and around intracranial arteriovenous malformations. Neurosurgery 2002;50:117–24. [PubMed: 11844242]

Krebs LT, Shutter JR, Tanigaki K, Honjo T, Stark KL, Gridley T. Haploinsufficient lethality and formation of arteriovenous malformations in Notch pathway mutants. Genes Dev 2004;18:2469–73. [PubMed: 15466160]

Kusaka N, Sugiu K, Katsumata A, Nakashima H, Tamiya T, Ohmoto T. The importance of venous hypertension in the formation of dural arteriovenous fistulas: a case report of multiple fistulas remote from sinus thrombosis. Neuroradiology 2001;43:980–4. [PubMed: 11760805]

Lawton MT, Jacobowitz R, Spetzler RF. Redefined role of angiogenesis in the pathogenesis of dural arteriovenous malformations. J Neurosurg 1997;87:267–74. [PubMed: 9254092]

Lyden D, Hattori K, Dias S, Costa C, Blaikie P, Butros L, Chadburn A, Heissig B, Marks W, Witte L, Wu Y, Hicklin D, Zhu Z, Hackett NR, Crystal RG, Moore MA, Hajjar KA, Manova K, Benezra R, Rafii S. Impaired recruitment of bone-marrow-derived endothelial and hematopoietic precursor cells blocks tumor angiogenesis and growth. Nat Med 2001;7:1194–201. [PubMed: 11689883]

Murphy PA, Lam MT, Wu X, Kim TN, Vartanian SM, Bollen AW, Carlson TR, Wang RA. Endothelial Notch4 signaling induces hallmarks of brain arteriovenous malformations in mice. Proc Natl Acad Sci U S A 2008;105:10901–6. [PubMed: 18667694]

Ng I, Tan WL, Ng PY, Lim J. Hypoxia inducible factor-1alpha and expression of vascular endothelial growth factor and its receptors in cerebral arteriovenous malformations. J Clin Neurosci. 2005

Nussbaum ES, Heros RC, Madison MT, Awasthi D, Truwit CL. The pathogenesis of arteriovenous malformations: insights provided by a case of multiple arteriovenous malformations developing in relation to a developmental venous anomaly. Neurosurgery 1998;43:347–51. [PubMed: 9696089]

Page-McCaw A, Ewald AJ, Werb Z. Matrix metalloproteinases and the regulation of tissue remodelling. Nat Rev Mol Cell Biol 2007;8:221–33. [PubMed: 17318226]

Park SO, Lee YJ, Seki T, Hong KH, Fliess N, Jiang Z, Park A, Wu X, Kaartinen V, Roman BL, Oh SP. ALK5- and TGFBR2-independent role of ALK1 in the pathogenesis of hereditary hemorrhagic telangiectasia type 2 (HHT2). Blood 2008;111:633–42. [PubMed: 17911384]

Petit I, Jin D, Rafii S. The SDF-1-CXCR4 signaling pathway: a molecular hub modulating neo-angiogenesis. Trends Immunol 2007;28:299–307. [PubMed: 17560169]

Philip M, Rowley DA, Schreiber H. Inflammation as a tumor promoter in cancer induction. Semin Cancer Biol 2004;14:433–9. [PubMed: 15489136]

Ping YF, Yao XH, Chen JH, Liu H, Chen DL, Zhou XD, Wang JM, Bian XW. The anti-cancer compound Nordy inhibits CXCR4-mediated production of IL-8 and VEGF by malignant human glioma cells. J Neurooncol 2007;84:21–9. [PubMed: 17415525]

Satomi J, Mount RJ, Toporsian M, Paterson AD, Wallace MC, Harrison RV, Letarte M. Cerebral vascular abnormalities in a murine model of hereditary hemorrhagic telangiectasia. Stroke 2003;34:783–9. [PubMed: 12624308]

Shin Y, Uranishi R, Nakase H, Sakaki T. [Vascular endothelial growth factor expression in the rat dural arteriovenous fistula model]. No To Shinkei 2003;55:946–52. [PubMed: 14727534]

Sure U, Battenberg E, Dempfle A, Tirakotai W, Bien S, Bertalanffy H. Hypoxiainducible factor and vascular endothelial growth factor are expressed more frequently in embolized than in nonembolized cerebral arteriovenous malformations. Neurosurgery 2004;55:663–9. [PubMed: 15335434]

Terada T, Higashida RT, Halbach VV, Dowd CF, Tsuura M, Komai N, Wilson CB, Hieshima GB. Development of acquired arteriovenous fistulas in rats due to venous hypertension. J Neurosurg 1994;80:884–9. [PubMed: 8169629]

Uranishi R, Nakase H, Sakaki T. Expression of angiogenic growth factors in dural arteriovenous fistula. J Neurosurg 1999;91:781–6. [PubMed: 10541235]

Xu B, Wu YQ, Huey M, Arthur HM, Marchuk DA, Hashimoto T, Young WL, Yang GY. Vascular endothelial growth factor induces abnormal microvasculature in the endoglin heterozygous mouse brain. J Cereb Blood Flow Metab 2004;24:237–44. [PubMed: 14747750]

Zhu Y, Lawton MT, Du R, Shwe Y, Chen Y, Shen F, Young WL, Yang GY. Expression of hypoxia-inducible factor-1 and vascular endothelial growth factor in response to venous hypertension. Neurosurgery 2006;59:687–96. [PubMed: 16955051]

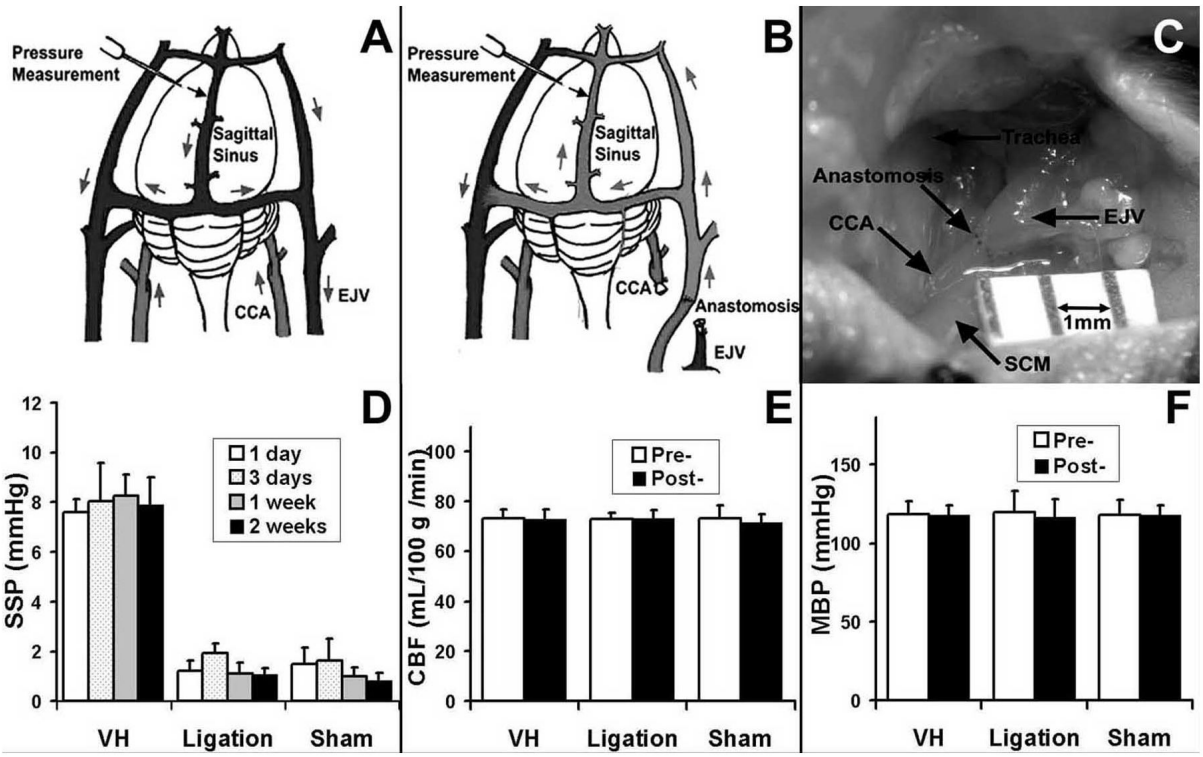

Figure 1. SSP pressure increased significantly in the VH brain

(A) Circulation of normal mouse brain. **(B)** Circulation of VH brain shows that CCA-EJV fistula (AVF) in the neck arterialized and pressurized the venous system. Arrows show direction of blood flow. **(C)** Photograph shows CCA-EJV anastomosis. SCM: Sternocleinomastoid muscle. Bar=1mm. **(D**) SSP. Creation of CCA-EJV fistula resulted in immediate and sustained increase of SSP. VH mice had constantly higher SSP pressure (8±1 mmHg) compared to CCA-ligation (1±1 mmHg, $p<0.05$) and sham groups (1±1 mmHg, $p<0.05$). **(E)** and **(F)** show that no significant changes for CBF and MBP were found pre- and post-operation in each group.

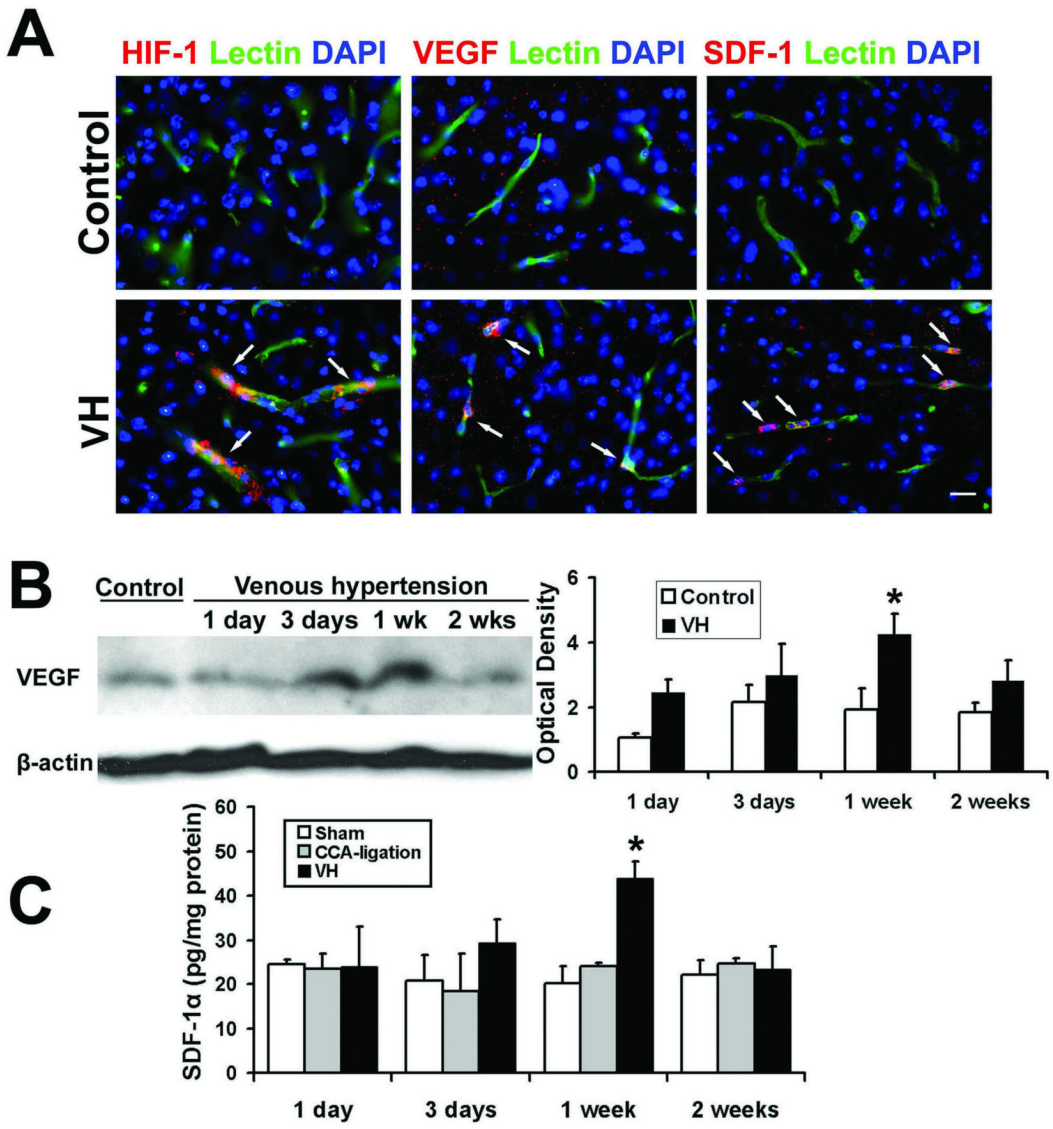

Figure 2. Increased HIF-1, VEGF and SDF-1 expression in the VH brain

(A) Photomicrographs show that HIF-1α, VEGF or SDF-1 expression was detected in the VH brain, but not in control brains (mice with CCA ligation). The expression of HIF-1α-, VEGF- or SDF-1-positive staining was localized to the endothelial cells (lectin staining, green) in vessel walls. The nuclei were counterstained with DAPI (blue). Scale Bar =20 μm. **(B)** Western blot analysis shows that VEGF expression increased in the VH brain. Image at left shows a representative Western blot. Minimal expression of VEGF was observed in the control group (CCA-ligation 1 week). Bar graph at right shows that VEGF expression increased 3 days and peaked 1 week after surgery (*p<0.05, compared with the CCA-ligation group). **(C)** Bar graph shows the results of ELISA analysis. The expression of SDF-1α began to increase at day 3, peaked at 1 week, and decreased 2 weeks post-operation. (*p<0.05, compared with the sham and CCA-ligation group)

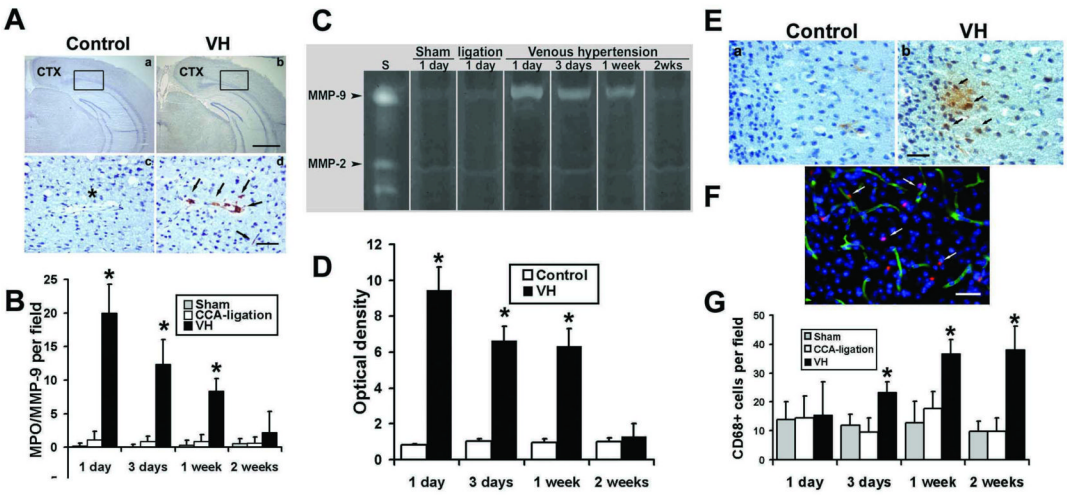

Figure 3. Increased leukocytes in the VH brain

(A) Photomicroimage of MPO-stained sections of the brains of VH (b and d) and control (a and c) groups. One day after surgery, the MPO positive signals (brown color) increased significantly in VH brains (d), which were mainly located in the parasagittal cortex (CTX). Enlarged pictures from the selected areas (d) show that neutrophils were mainly located in the vascular wall. The nuclei were counterstained with hematoxylin. Neutrophils were absent in the brain tissue from the control groups (a and c). * in c indicates a similar-sized vessel in d. Scale bars for a and b are 1000 μm; for c and d, 50 μm. **(B)** Bar graph shows neutrophil counting. (*$p<0.05$, compared with the control group). **(C)** Increased expression of MMP-9 in the VH brain illustrated by gelatin zymogram gel image. S: MMP standards. Low level of MMP-9 activity was detected in the brains of control groups (Sham and CCA ligation) at day 1 after surgery. MMP-9 activity greatly increased in the VH brains day 1 after the surgery. **(D)** Bar graph shows the time course of MMP-9 expression. MMP-9 activity was highest at day 1 post operation, and then returned to the baseline 2 weeks after surgery. The time course of MMP-9 expression coincided with the infiltration of neutrophils. MMP-2 was expressed equally in all the groups at all time points. The control sample is from CCA-ligation group. (*$p<0.05$, compared with the control groups). **(E)** Photomicroimage shows macrophage infiltration in the parasagittal cortex of the VH brain 3 days after surgery. CD68 positive cells stained in brown color. There were few macrophages in CCA-ligation brains (a), whereas many macrophages were detected either in the vessel wall or in the parenchyma of VH brains (b). The nuclei were counterstained with hematoxylin. Scale bar = 40 μm. **(F)** Double fluorescence staining of CD68 (red) and Lectin (green) show that macrophage was localized in the vessel wall or in parenchyma. The nuclei were counterstained with DAPI. **(G)** Bar graph shows quantification of macrophages at different time points. Macrophages began to increase at day 3, and gradually increased and plateaued 1 week following surgery. The time course of macrophage infiltration coincided with increased SDF-1 expression. (*$p<0.05$, compared with the sham or ligation group)